*Aust. J. Phys.*, 1986, **39**, 513–27

# The Influence of the Spatial Harmonics on the Rotating Magnetic Field Current Drive

*W. N. Hugrass*

Los Alamos National Laboratory, University of California,
Los Alamos, NM 87545, U.S.A.

*Abstract*

In rotating magnetic field (RMF) current drive experiments, the RMF is usually generated by means of a two-phase radio frequency (r.f.) system which feeds a pair of orthogonal coils. The magnetic field generated in this manner consists of the desired RMF as well as the (undesired) odd spatial harmonics. The $(2j-1)$th spatial harmonic field rotates about the axis at an angular speed $(-1)^{j-1}\omega/(2j-1)$, where $\omega$ is the angular frequency of the r.f. current. In order to evaluate the effect of these spatial harmonics on the performance of the RMF current drive experiments, we have developed a simplified theoretical model for the plasma. In this model, the ions are assumed immobile and the motion of the electron fluid in the azimuthal direction is assumed to be a rigid rotation. It has been found using this model that the presence of the spatial harmonics makes the RMF current drive less efficient. It has also been found that the effect of the spatial harmonics can be made negligible by (a) making the width of the coils sufficiently larger than the diameter of the plasma, (b) carefully designing the coil configuration to eliminate the fifth harmonic or (c) using a three-phase system to generate the RMF.

## 1. Introduction

In RMF current drive experiments, a steady azimuthal current is driven in the plasma by means of a rotating magnetic field. This RMF is usually generated by using a two-phase r.f. source to feed two sets of orthogonal coils (see e.g. Blevin and Thonemann 1962; Hugrass *et al.* 1981; Durance *et al.* 1982). The magnetic fields generated in these practical situations consist of the desired RMF as well as the odd spatial harmonics of this field; the $(2j-1)$th spatial harmonic field rotates about the axis at an angular frequency $(-1)^{j-1}\omega/(2j-1)$, where $\omega$ is the angular frequency of the r.f. current. Nevertheless, it has been assumed in the previous theoretical investigations that a 'pure' RMF was applied to the plasma (Blevin and Thonemann 1962; Jones and Hugrass 1981; Hugrass and Grimm 1981; Hugrass 1982*a*). The purpose of the present work is to estimate the influence of the spatial harmonics on the RMF current drive. It is extremely difficult to study the effect of these harmonics using an elaborate model for the plasma. We, therefore, have developed an approximate model for the plasma where the motion of the ion fluid is neglected and the motion of the electron fluid in the azimuthal direction is assumed to be a rigid rotation. Our assumptions, with the exception of the rigid rotation condition, are identical to the immobile ion model (Jones and Hugrass 1981). This extra assumption leads to a great simplification of the analysis and makes the concept easier to grasp

0004-9506/86/040513$02.00

without sacrificing much of the accuracy. By adopting this model, and making use of the analogy between the RMF technique of current drive and the operation of the induction motor (Hugrass 1984), the study of the influence of the spatial harmonics on the RMF current drive has been made straightforward. The results obtained in this paper show that the spatial harmonics have, in general, an adverse effect. It is also shown that the effect of the spatial harmonics can be made negligible by carefully designing the coils and/or using a three-phase r.f. system to generate the RMF.

The formulae for the magnetic field generated by infinitely long polyphase systems are given in Section 2. In Section 3 the simplified model for the plasma is used to calculate the torque exerted on the electron fluid by a single spatial harmonic component. The results obtained in Sections 2 and 3 are used in Section 4 to calculate the total torque applied on the electron fluid by the magnetic field generated using two-phase and three-phase systems. The effect of the spatial harmonics on the efficiency of the RMF current drive is considered in Section 5 and the results are discussed in Section 6.

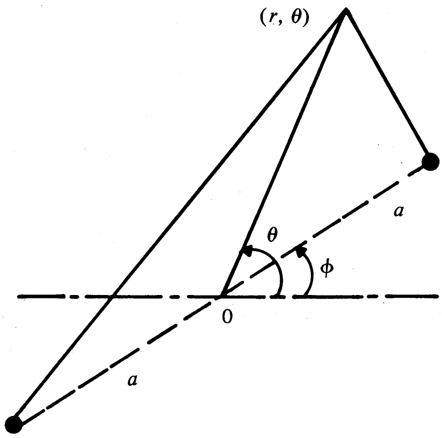


**Fig. 1.** Coordinate system for the calculation of the vector potential of an infinitely long dipole. Note that the $z$-axis is perpendicular to the plane; $r$, $\theta$ and $z$ are the standard cylindrical coordinates.

## 2. Magnetic Field Generated by Polyphase Systems

In this section we consider the magnetic field generated by means of polyphase currents flowing in a set of infinitely long dipole coils arranged on a cylindrical surface of radius $a$. The vector potential of a dipole coil located at an angle $\phi$ (see Fig. 1) is given by

$$A_z = \frac{\mu_0 I}{4\pi} \ln\left(\frac{1 + r^2/a^2 - 2(r/a)\cos(\theta - \phi)}{1 + r^2/a^2 + 2(r/a)\cos(\theta - \phi)}\right). \tag{1}$$

In the region $0 \leqslant r \leqslant a$, the vector potential can be expanded into

$$A_z = -\frac{\mu_0 I}{\pi} \sum_{j=1}^{\infty} \frac{1}{2j-1}\left(\frac{r}{a}\right)^{2j-1} \cos\{(2j-1)(\theta - \phi)\}. \tag{2}$$

For a general polyphase winding we consider a number of dipole coils; the $i$th dipole is located at an angular position $\phi_i$ and carries a current

$$I_i = I \sin(\omega t - \zeta_i). \tag{3}$$

The simplest two-phase system consists of two orthogonal coils, located at $\phi_1 = 0$ and $\phi_2 = \pi/2$, and carrying the currents $I_1 = -I_0 \sin\omega t$ and $I_2 = -I_0 \sin(\omega t - \frac{1}{2}\pi)$. It follows that

$$A_z = -\frac{\mu_0 I_0}{\pi} \sum_{j=1}^{\infty} \frac{1}{2j-1} \left(\frac{r}{a}\right)^{2j-1} \sin\{\omega t + (-1)^j (2j-1)\theta\}. \tag{4}$$

Using the relationship $\nabla \times \boldsymbol{A} = \boldsymbol{B}$, we obtain

$$B_r = \frac{\mu_0 I_0}{\pi a} \sum_{j=1}^{\infty} (-1)^{j-1} \left(\frac{r}{a}\right)^{2j-2} \cos\{\omega t + (-1)^j (2j-1)\theta\}, \tag{5}$$

$$B_\theta = \frac{\mu_0 I_0}{\pi a} \sum_{j=1}^{\infty} \left(\frac{r}{a}\right)^{2j-2} \sin\{\omega t + (-1)^j (2j-1)\theta\}. \tag{6}$$

We note that the magnetic field consists of a fundamental ($j = 1$) component, which rotates about the axis at an angular velocity $\omega$, and the odd spatial harmonics. The $(2j-1)$th harmonic component rotates about the axis at an angular velocity $(-1)^{j-1}\omega/(2j-1)$. As shown later in this paper, the presence of these spatial harmonics can have a harmful effect on RMF current drive systems. It is, therefore, desirable to design the polyphase windings so that the relative magnitudes of the spatial harmonics are minimised. It is obvious that the relative magnitudes of the harmonics in the region occupied by the plasma ($r \leqslant R$) can be reduced by making the coil width much larger than the diameter of the plasma (i.e. $2a \gg 2R$). It is also possible to decrease the relative magnitudes of the spatial harmonics by using more than one coil for each phase or by using a larger number of phases. For a two-phase system with two coils per phase one obtains

$$A_z = -\frac{2\mu_0 I_0}{\pi} \sum_{j=1}^{\infty} \frac{\cos\{\frac{1}{2}(2j-1)\alpha\}}{2j-1} \left(\frac{r}{a}\right)^{2j-1} \sin\{\omega t + (-1)^j (2j-1)\theta\}, \tag{7}$$

where $\alpha$ is the angular spacing between the two coils pertaining to each phase. It is seen that the relative magnitude of the $(2j-1)$th harmonic is reduced by the factor $\cos\{\frac{1}{2}(2j-1)\alpha\}/\cos\frac{1}{2}\alpha$. One may choose $\alpha = \pi/4$ so that eight conductors corresponding to the four dipole coils are equally spaced in the azimuthal direction.

For a three-phase system with one conductor per phase consisting of three dipole coils located at $\phi = 0$, $\pi/3$ and $2\pi/3$ and carrying current with phase angles $\zeta = 0$, $\pi/3$ and $2\pi/3$, one obtains

$$A_z = -\frac{3\mu_0 I_0}{2\pi} \sum_{j=1}^{\infty} \frac{1}{2j-1} \left(\frac{r}{a}\right)^{2j-1} \gamma_j \sin\{\omega t - \beta_j (2j-1)\theta\}, \tag{8}$$

where $\gamma_1 = 1$, $\gamma_2 = 0$, $\gamma_3 = 1$ and $\gamma_{j+3} = \gamma_j$ and $\beta_1 = 1$, $\beta_3 = -1$ and $\beta_{j+3} = \beta_j$.

The vector potential for a three-phase system with two conductors per phase is

$$A_z = -\frac{3\mu_0 I_0}{\pi}\sum_{j=1}^{\infty}\frac{\cos\{\frac{1}{2}(2j-1)\alpha\}}{2j-1}\left(\frac{r}{a}\right)^{2j-1}\gamma_j\sin\{\omega t-\beta_j(2j-1)\theta\}\,. \tag{9}$$

It is seen that the 3rd, 9th, 15th, ... harmonic components are not present and that the 1st, 7th, 13th, ... harmonic components rotate in one direction, while the 5th, 11th, 17th ... harmonic components rotate in the opposite direction.

## 3. Generalised Induction Motor Model

The analogy between the RMF current drive and the operation of the induction motor (Hugrass 1984) has proved to be a useful tool both in explaining the physical mechanisms involved in the RMF current drive and in predicting some of the subtle features of this current drive technique (Hugrass 1985). In this section, this analogy will be generalised in two respects. Firstly, the inductance–resistance ($L$–$R$) circuit model adopted in the earlier work is replaced by a more elaborate model. And secondly, we extend the analysis to describe RMF current drive by means of a rotating field configuration with an arbitrary value of $m$ (the number of poles is $2m$).

We consider an infinitely long cylindrical plasma of radius $a$. The ions are assumed to be infinitely massive and to have a uniform density. The electrons are assumed to form a massless cold fluid. We further assume that the motion of the electron fluid in the azimuthal direction is a rigid rotation; the azimuthal component of the electron fluid velocity is

$$v_\theta = \omega_r\, r\,, \tag{10}$$

where $\omega_r$ is a constant. It is also assumed that the radius of the plasma is much smaller than the free space wavelength associated with the frequency of the RMF, hence the displacement current can be neglected. The fields and currents satisfy Maxwell's equations

$$\nabla\times\boldsymbol{E} = -\partial\boldsymbol{B}/\partial t\,, \qquad \nabla\times\boldsymbol{B} = \mu_0\,\boldsymbol{J} \tag{11, 12}$$

and Ohm's law

$$\eta\boldsymbol{J} = \boldsymbol{E}-(1/ne)\boldsymbol{J}\times\boldsymbol{B}\,, \tag{13}$$

where $n$ is the number density and the current density $\boldsymbol{J}$ is related to the velocity of the electron fluid by

$$\boldsymbol{J} = -ne\boldsymbol{v}_{\mathrm{e}}\,. \tag{14}$$

To this cylindrical plasma, an RMF is applied. The vector potential associated with this field is

$$A_z = \mathrm{Re}\left\{\frac{\mathrm{i}aB_m}{m}\left(\frac{r}{a}\right)^m \mathrm{e}^{\mathrm{i}(\omega t-m\theta)}\right\}, \tag{15}$$

where $B_m$ is the magnitude of the RMF at $r = a$ (in the absence of the plasma).

From now on we adopt the standard phasor notation. For example, $A_z$, $B_r$ and $J_z$ will denote the complex amplitudes of these quantities. It can be shown that the $z$ component of the electric field satisfies

$$r^2 \frac{d^2 E_z}{d r^2} + r \frac{d E_z}{d r} - (m^2 + \alpha_m^2 r^2) E_z = 0, \tag{16}$$

where $\alpha_m^2 = 2i/\delta_m^2$ and $\delta_m$ is the Doppler shifted skin depth defined by

$$\delta_m^2 = 2\eta/\omega\mu_0 S_m, \tag{17}$$

and $S_m$ is the slip factor

$$S_m = (\omega - m\omega_r)/\omega. \tag{18}$$

The solution to equation (16), which is finite at $r = 0$, continuous at $r = a$ and tends to the externally applied field at $r \gg a$, is given by

$$E_z = \frac{2\omega}{\alpha_m} B_m \frac{I_m(\alpha_m r)}{I_{m-1}(\alpha_m a)}, \tag{19}$$

where $I_m$ is the modified Bessel function of order $m$. All the other field and current components can be obtained in terms of $E_z$ using equations (11) and (12). The torque (per unit length) applied by the RMF on the electron fluid is given by

$$\begin{aligned} T_m &= \tfrac{1}{2} \int_0^a 2\pi r^2 J_z^* B_r \, d r \\ &= 2\pi m \delta_m^2 \frac{B_m^2}{\mu_0} \frac{\operatorname{ber}_m(x) \operatorname{bei}'_m(x) - \operatorname{ber}'_m(x) \operatorname{bei}_m(x)}{\operatorname{ber}^2_{m-1}(x) + \operatorname{bei}^2_{m-1}(x)}, \end{aligned} \tag{20}$$

where the argument of the Kelvin functions is $x = \sqrt{2}\, a/\delta_m$. Equation (20) can be written in a more convenient form by expanding the products of the Kelvin functions into power series:

$$T_m = \frac{\pi \omega a^4 B_m^2 S_m}{2m(m+1)\eta} \frac{\Sigma \zeta_j}{\Sigma \xi_j}, \tag{21}$$

where $\zeta_1 = \xi_1 = 1$ and

$$\zeta_{j+1} = \frac{x^4 \zeta_j}{16j(m+j)(m+2j)(m+2j+1)},$$

$$\xi_{j+1} = \frac{x^4 \xi_j}{16j(m+j-1)(m+2j-2)(m+2j-1)}.$$

Note that the torque is in the same rotational direction as the $m$th component of the rotating field for $\omega_r < \omega/m$ and is in the opposite direction for $\omega_r \geqslant \omega/m$.

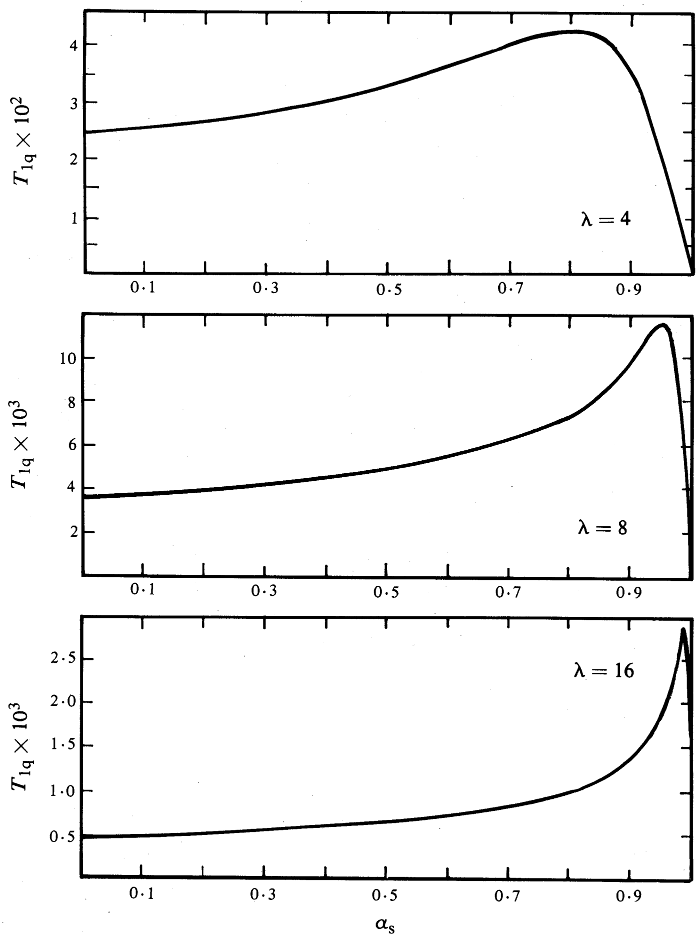


**Fig. 2.** (*a*) Normalised torque $T_{1q}$ plotted against the normalised frequency of rotation $\alpha_s$ for a system with pure RMF ($k = 0$) and for $\lambda = 4$, 8 and 16; (*b*) the corresponding $\alpha_s$ versus $\gamma_1$ curves.

## 4. RMF Current Drive with Practical Coil Configurations

We now use the results obtained in Sections 2 and 3 to calculate the steady state azimuthal d.c. current driven in a unit length of a cylindrical plasma by means of the RMF generated using a number of practical coil configurations. We note that, in the steady state, the torque applied on the electron fluid by the RMF is exactly balanced by the retarding torque $T_c$, which arises from the electron–ion collisions,

$$T_c = \int_0^a 2\pi r^2 n m_e v_{e\theta} \nu_{ei} \, dr = \tfrac{1}{2}\pi n m_e \nu_{ei} \omega_r a^4 , \tag{22}$$

where $m_e$ is the electron mass and $\nu_{ei}$ is the electron–ion collision frequency. Considering equations (21) and (22) and recalling the classical formula $\eta = m_e \nu_{ei}/ne^2$,

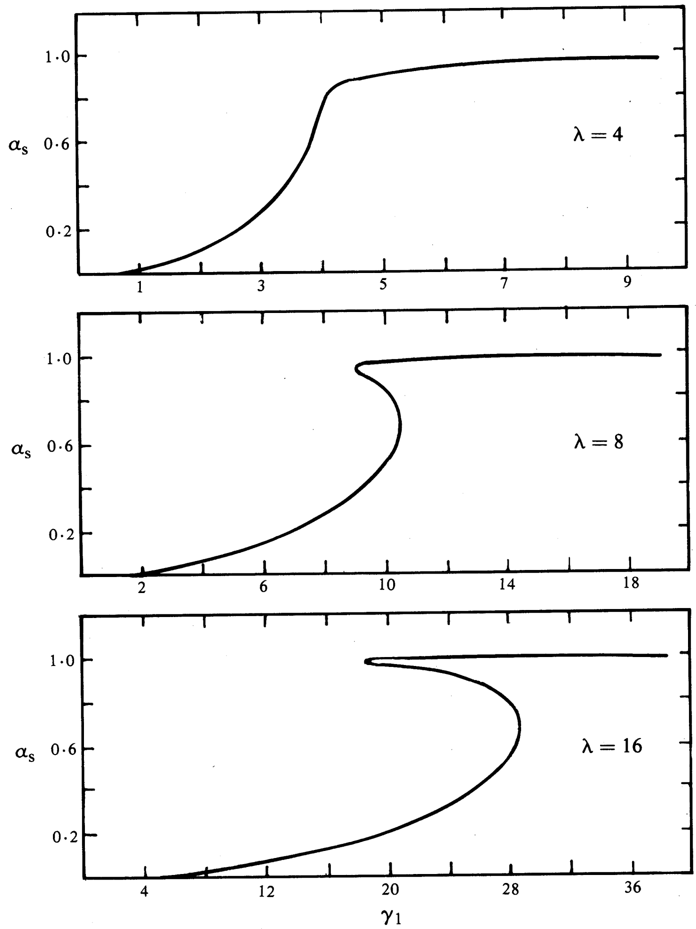


**Fig. 2*b*.**

one finds that the analysis can be simplified by normalising the torque to the quantity

$$T_q = \frac{\pi}{2} \frac{ne^2}{m_e \nu_{ei}} \omega a^4 B_{\omega 1}^2, \tag{23}$$

where $B_{\omega 1}$ is the magnitude of the fundamental component of the RMF. Equations (21) and (22) can now be written in the normalised form

$$T_{mq} = \left(\frac{B_m}{B_{\omega 1}}\right)^2 \frac{S_m}{m(m+1)} \frac{\Sigma \zeta_j}{\Sigma \xi_j}, \qquad T_{cq} = \frac{1}{\gamma_1^2} \frac{\omega_r}{\omega}, \tag{24, 25}$$

where

$$\gamma_1 = \frac{eB_{\omega 1}}{m_e \nu_{ei}} = \frac{\omega_{ce1}}{\nu_{ei}}. \tag{26}$$

The analysis presented so far shows that the performance of an RMF current drive system (as described by our simplified model) is determined by three dimensionless parameters: $k$, the ratio of the diameter of the plasma cylinder to the width of the coils; $\lambda$, the ratio of the plasma radius to the classical skin depth $\delta = (2\eta/\mu_0\,\omega)^{\frac{1}{2}}$; and $\gamma_1 = \omega_{ce1}/\nu_{ei}$. These three parameters are sufficient to determine the normalised angular velocity of the electron fluid $\alpha_s = \omega_r/\omega$ which, in this model, is equal to the ratio of the steady azimuthal current to the maximum possible value of this current corresponding to the electron fluid rotating synchronously with the RMF.

The performance of the RMF current drive systems is customarily evaluated by considering the $\alpha_s$ versus $\gamma_1$ characteristics (see e.g. Hugrass 1985); here we follow this conventional approach. We obtain the torque in terms of $\alpha_s$ using equations (18) and (24). The $\alpha_s$ versus $\gamma_1$ characteristics are then obtained by equating this applied torque to the 'load' torque (equation 25). We start by considering systems with 'pure' RMF ($k = 0$ in this model). Fig. 2$a$ shows the normalised torque plotted against the normalised frequency for $\lambda = 4$, 8 and 16, and Fig. 2$b$ shows the corresponding $\alpha_s$ versus $\gamma_1$ curves. We note that, for a pure RMF, the predictions of this simple model are qualitatively similar to those obtained using other models (Hugrass 1985). In practical systems, however, the ratio of the plasma diameter to the width of the dipole coils is $0\cdot5 < k < 0\cdot8$. It follows that the magnitudes of the spatial harmonics are not much smaller than that of the fundamental component and the pure RMF approximation can lead to erroneous conclusions. Fig. 3$a$ shows the normalised torque applied by the fundamental RMF field, the third and the fifth harmonics as well as the total normalised torque, plotted against the normalised frequency for $\lambda = 8$ and $k = 0\cdot8$. In the steady state the total torque applied by the field is equal to the retarding torque; one, therefore, can use Fig. 3$a$ to construct the $\alpha_s$ versus $\gamma_1$ curve for this case (see Fig. 3$b$). It is seen that the performance of the system for $\lambda = 8$ and $k = 0\cdot8$ is qualitatively different from that for $\lambda = 8$ and $k = 0$ in Fig. 2. For $\gamma_1 \gg 8$ there are three possible steady state solutions; the solution with the smallest value of $\alpha_s$ ($\approx 0\cdot2$) is the actual steady state solution obtained for a system starting from a zero initial rotational velocity. It is seen from Fig. 3$a$ that the normalised driven current is clamped to $\alpha_s \approx 0\cdot2$ because the total torque is negative for $\alpha_s$ slightly larger than $0\cdot2$. This, in turn, arises from the large negative torque applied by the fifth harmonic field which is synchronous with the electron fluid for $\alpha_s = 0\cdot2$. The fact that total torque is negative over a certain range of $\omega_r$ may seem paradoxical; however, it is a physically valid result. The field generated by means of practical polyphase windings is not a pure mode rotating field, but consists of a number of modes rotating at different angular velocities. Bearing this in mind, it is not surprising that the total torque can be negative for certain values of $\omega_r$, especially for $\omega_r \geqslant \omega/5$. In fact, even for a pure rotating field, the torque is negative for $\omega_r > \omega$.

It is obvious that the effect of the spatial harmonics on the performance of the system can be made less pronounced by making the width of the dipole coils sufficiently larger than the diameter of the plasma cylinder. Fig. 4 shows the characteristics of an RMF current drive system for $\lambda = 8$ and $k = 0\cdot7$. It is seen that the $\alpha_s$ versus $\gamma_1$ curve is qualitatively similar to the corresponding curve for a pure RMF system ($k = 0$). One can conclude that for a given value of $\lambda$, there exists a critical value of $k$ above which the performance of an RMF current drive system is strongly influenced by the spatial harmonics. Fig. 5 shows the characteristics of the RMF

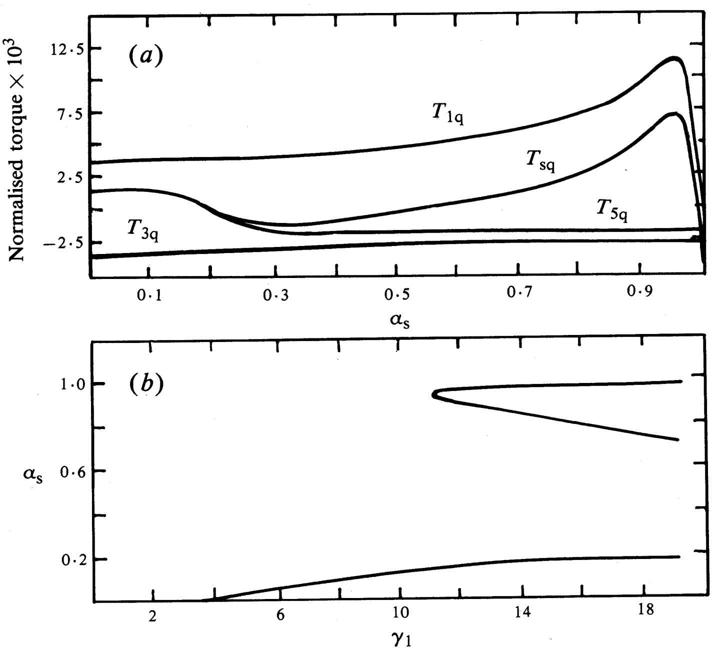


**Fig. 3.** (*a*) Normalised torque applied by the fundamental, third and fifth harmonics and the total normalised torque plotted against $\alpha_s$ for a two-phase system and for $\lambda = 8$ and $k = 0{\cdot}8$; (*b*) the corresponding $\alpha_s$ versus $\gamma_1$ curve.

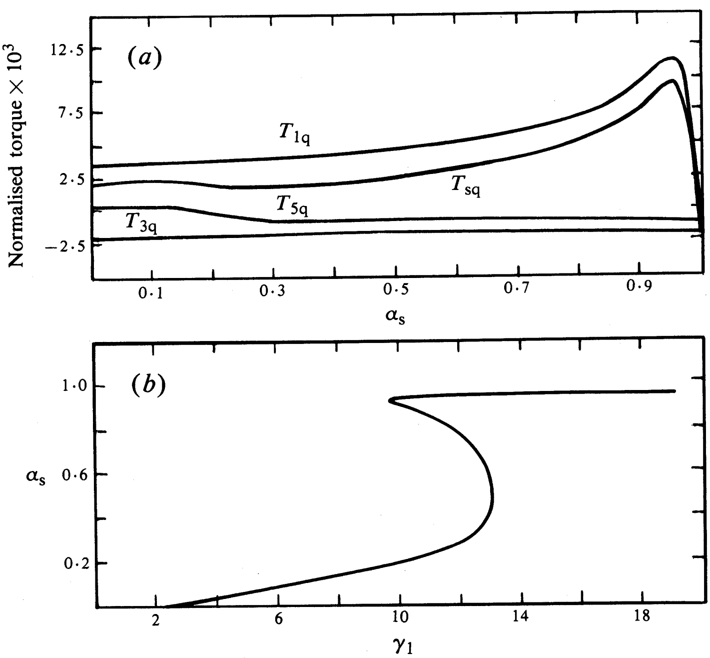


**Fig. 4.** (*a*) Normalised torque applied by the fundamental, third and fifth harmonics and the total normalised torque plotted against $\alpha_s$ for a two-phase system and for $\lambda = 8$ and $k = 0{\cdot}7$; (*b*) the corresponding $\alpha_s$ versus $\gamma_1$ curve.

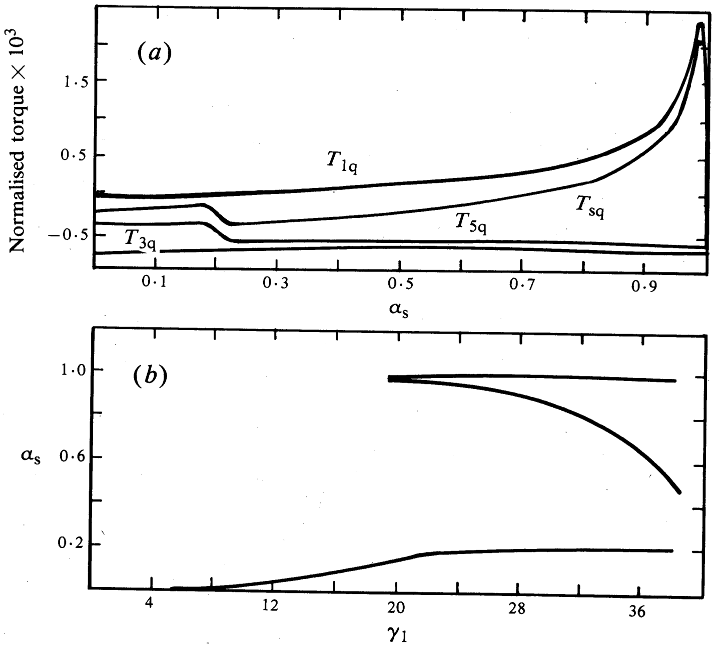


**Fig. 5.** (*a*) Normalised torque applied by the fundamental, third and fifth harmonics and the total normalised torque plotted against $\alpha_s$ for a two-phase system and for $\lambda = 16$ and $k = 0{\cdot}7$; (*b*) the corresponding $\alpha_s$ versus $\gamma_1$ curve.

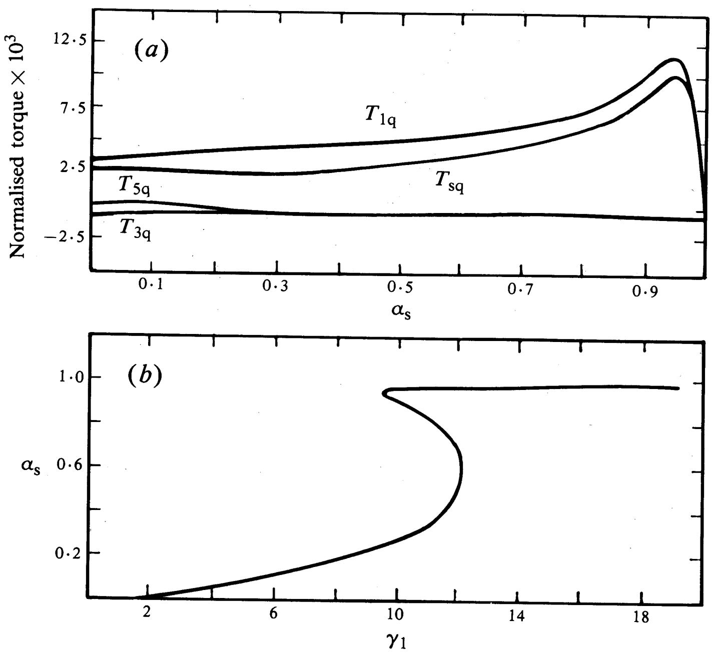


**Fig. 6.** (*a*) Normalised torque applied by the fundamental, third and fifth harmonics and the total normalised torque plotted against $\alpha_s$ for a two-phase system with two coils per phase spaced at $\pi/4$ and for $\lambda = 8$ and $k = 0{\cdot}8$; (*b*) the $\alpha_s$ versus $\gamma_1$ curve for $\lambda = 8$ and $k = 0{\cdot}8$.

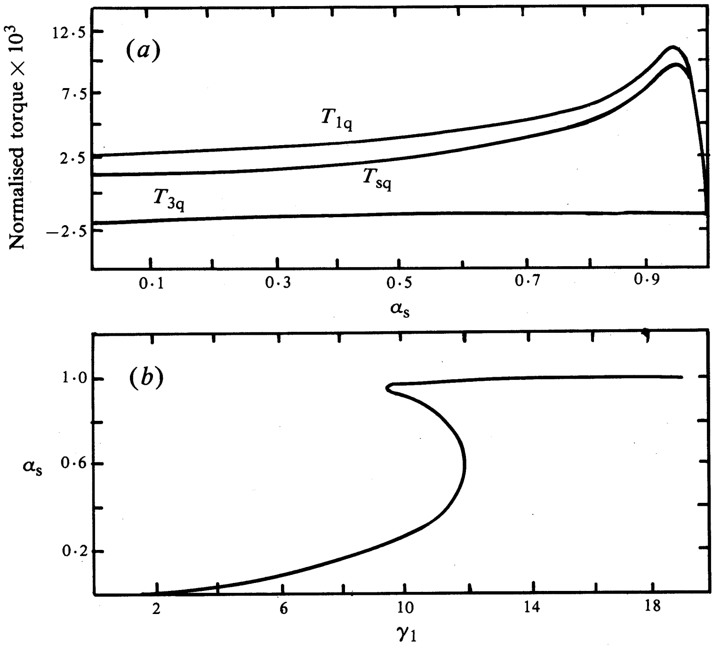


**Fig. 7.** (*a*) Normalised torque applied by the fundamental and third harmonics and the total normalised torque plotted against $\alpha_s$ for a two-phase system with two coils per phase spaced at $\pi/5$ and for $\lambda = 8$ and $k = 0 \cdot 8$; (*b*) the $\alpha_s$ versus $\gamma_1$ curve for $\lambda = 8$ and $k = 0 \cdot 8$.

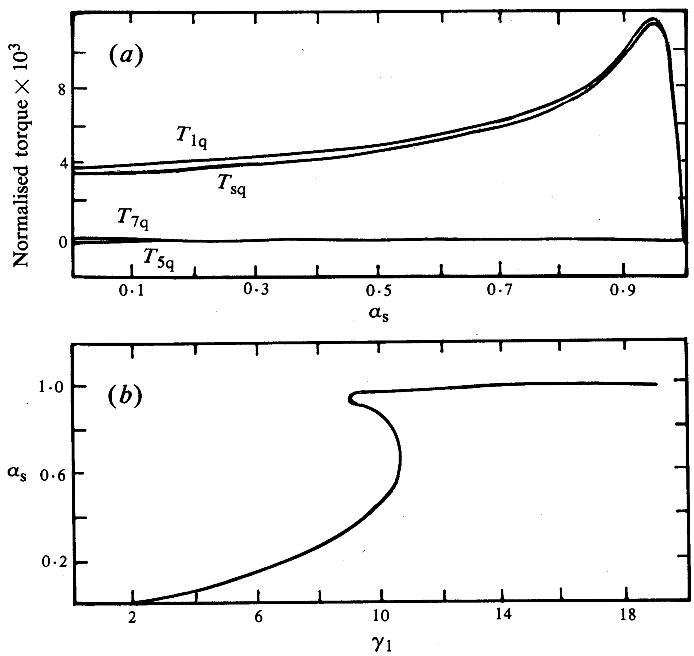


**Fig. 8.** (*a*) Normalised torque applied by the fundamental, fifth and seventh harmonics and the total normalised torque plotted against $\alpha_s$ for a three-phase system with two coils per phase spaced at $\pi/6$ and for $\lambda = 8$ and $k = 0 \cdot 8$; (*b*) the $\alpha_s$ versus $\gamma_1$ curve for $\lambda = 8$ and $k = 0 \cdot 8$.

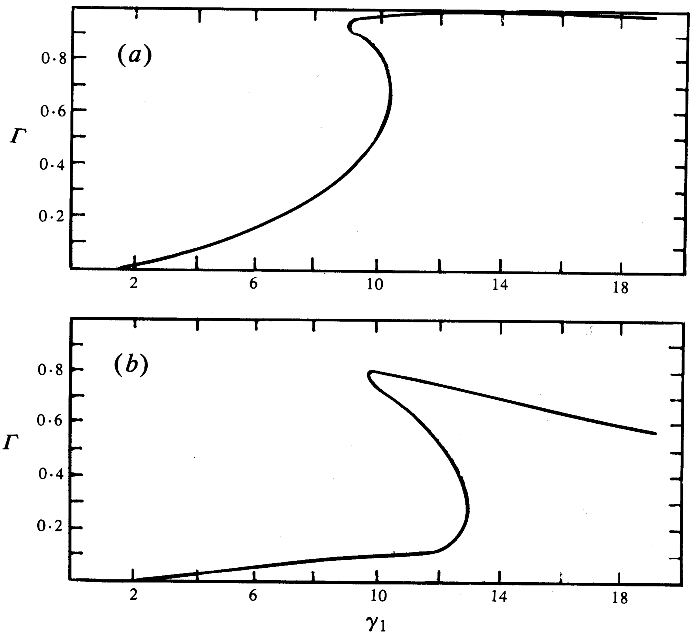


**Fig. 9.** Efficiency $\Gamma$ plotted against $\gamma_1$ for $\lambda = 8$ and for (*a*) a pure RMF; (*b*) a two-phase system with one coil per phase and $k = 0 \cdot 7$; (*c*) a two-phase system with one coil per phase and $k = 0 \cdot 8$; (*d*) a two-phase system with two coils per phase (spaced at $\pi/4$) and $k = 0 \cdot 8$; and (*e*) a three-phase system with two coils per phase (spaced at $\pi/6$) and $k = 0 \cdot 8$.

current drive for $\lambda = 16$ and $k = 0 \cdot 7$. By comparing Figs 4 and 5, it is seen that the critical value of $k$ is smaller for larger values of $\lambda$.

It is also possible to minimise the effect of the spatial harmonics by using two dipole coils per phase. As stated in Section 2, the angle between the two dipole coils pertaining to the same phase can be made either equal to $\pi/4$, so that the eight sides of the coils are equally spaced in the azimuthal direction, or it can be made equal to $\pi/5$ so that the potentially harmful fifth harmonic vanishes. Figs 6 and 7 show the characteristics of RMF systems utilising two-phase r.f. sources and having two coils per phase, for $\lambda = 8$ and $k = 0 \cdot 8$, for angular spacings of $\pi/4$ and $\pi/5$ respectively. It is possible to achieve further improvement by using a three-phase r.f. source. In this case the seventh spatial harmonic is potentially the most harmful. Fig. 8 shows the characteristics for an RMF system utilising a three-phase r.f. source feeding two coils per phase (the angle between the two coils corresponding to the same phase is $\pi/6$) for $\lambda = 8$ and $k = 0 \cdot 8$. It is seen that the effect of the spatial harmonics on the system is negligible for this case.

## 5. Efficiency of the RMF Current Drive

The efficiency of the RMF current drive has been the subject of controversy in the literature in the last few years. Fisch and Watanabe (1982) used a particle orbit model to calculate the efficiency of the RMF current drive, and concluded that it was a very inefficient technique. It was shown later (Hugrass 1982*b*), using the global conservation laws derived from Maxwell's equations (Klima 1973, 1974), that the

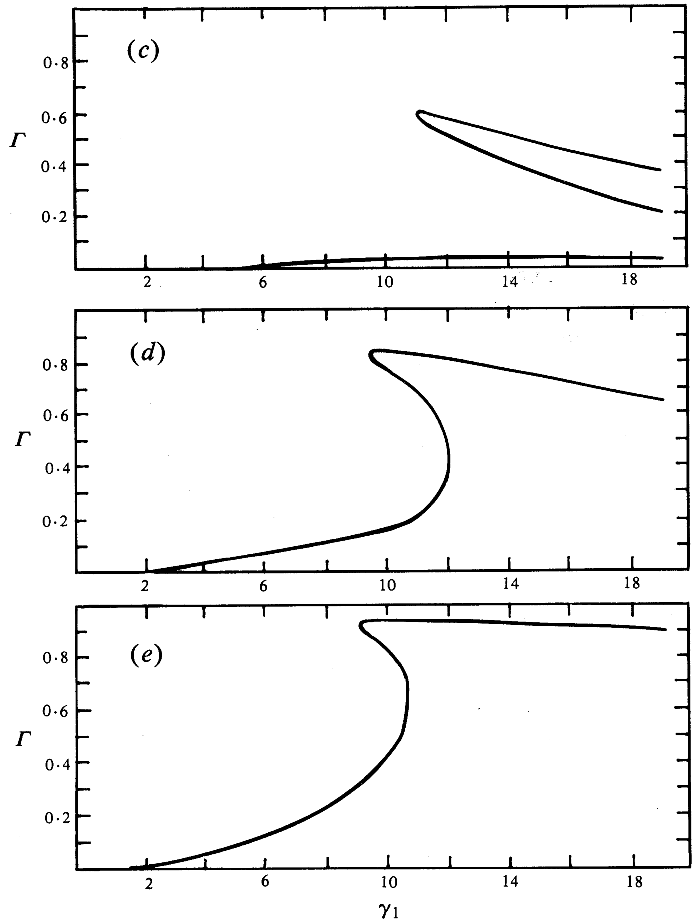


**Figs 9*c–e*.**

efficiency of the RMF current drive technique is very high because the phase velocity of the RMF is not much greater than the electron drift velocity. Recently, Kaw and Sen (1986) used a fluid model to calculate the efficiency of the RMF current drive. Their conclusions are in agreement with those obtained using the global conservation laws (Hugrass 1982*b*, 1984) in the limit where the magnitude of the RMF is much smaller than the equilibrium field. It is shown later in this section that the predictions of our simplified model are in complete agreement with the global conservation laws.

We define the efficiency of the RMF current drive $\Gamma$ as the ratio of the Joule dissipation per unit length associated with the driven d.c. azimuthal current $P_{\mathrm{dc}}$, to the power per unit length transferred from the r.f. source to the plasma $P_{\mathrm{rf}}$. Using equations (20) and (22) and the relationship $E_{zm} = (\omega/m)rB_{rm}$, it can be shown that

$$P_{\mathrm{dc}} = \int_0^a 2\pi r\eta J_{\mathrm{dc}}^2 \,\mathrm{d}r = \tfrac{1}{2}\pi\eta e^2 a^4 \omega_r^2 = \omega_r T_{\mathrm{c}}, \tag{27}$$

$$P_{\mathrm{rf}} = \tfrac{1}{2}\int_0^a 2\pi r J_z^* E_z \,\mathrm{d}r = \sum_j (-1)^{j-1} \frac{\omega}{2j-1} T_{2j-1}. \tag{28}$$

We also note that equation (28) can be derived directly from the Klima (1974) theorem. In the steady state we have $T_c = \Sigma\, T_{2j-1}$; it follows that

$$\Gamma = \frac{P_{dc}}{P_{rf}} = \frac{\omega_r}{\omega}\Big(\sum_j T_{2j-1}\Big)\Big/\Big(\sum_j \frac{(-1)^{j-1}}{2j-1}\, T_{2j-1}\Big). \tag{29}$$

We note that equations (28) and (29) are written for a two-phase system. The corresponding equations for a three-phase system are similar.

Fig. 9 shows the efficiency $\Gamma$ plotted against $\gamma_1$ for $\lambda = 8$ and for the five cases listed. We see that, for $k = 0\cdot 8$, the efficiency of the system is much less than for a pure RMF system, whereas the effect of the spatial harmonics is less significant for $k = 0\cdot 7$. It is also seen that the three-phase system is almost as efficient as the pure RMF system.

## 6. Discussion and Conclusions

We have shown that the magnetic field generated by means of the practical polyphase systems consists of the desired RMF component as well as the spatial harmonic fields. These spatial harmonics can severely impair the performance of the system; however, it is also shown that the effect of these harmonics can be made negligible by (a) making the width of the dipole coils sufficiently larger than the diameter of the plasma, (b) carefully designing the coils to minimise the relative magnitude of the harmonic fields or (c) using a three-phase system. These conclusions were obtained using a very simplified model for the plasma. It should be pointed out that our model has the following limitations: (1) the motion of the ion fluid and the compressible oscillations that may arise from it are neglected; (2) the motion of the electron fluid in the azimuthal direction is assumed to be a rigid rotation; and (3) we have assumed an infinitely long cylindrical plasma, whereas the plasma equilibria obtained in many RMF experiments are oblate compact toroids (Durance *et al.* 1982)—the end effects should be appreciable in such experiments. We think, however, that the predictions obtained using this simple model are qualitatively correct and may provide some useful guidelines for the design of future RMF experiments.

## Acknowledgments

This work has been supported by the U.S. Department of Energy. The author was a NERDDC Fellow at The Flinders University of South Australia during the early stages of this work. Many useful discussions with Professor I. R. Jones are acknowledged.

## References

Blevin, H. A., and Thonemann, P. C. (1962). *Nucl. Fusion Suppl.* Part 1, p. 55.
Durance, G., Jessup, B. L., Jones, I. R., and Tendys, J. (1982). *Phys. Rev. Lett.* **48**, 1253.
Fisch, N. J., and Watanabe, T. (1982). *Nucl. Fusion* **22**, 423.
Hugrass, W. N. (1982*a*). *J. Plasma Phys.* **28**, 369.
Hugrass, W. N. (1982*b*). *Nucl. Fusion* **22**, 1237.
Hugrass, W. N. (1984). *Aust. J. Phys.* **37**, 509.

Hugrass, W. N. (1985). *Aust. J. Phys.* **38**, 157.
Hugrass, W. N., and Grimm, R. C. (1981). *J. Plasma Phys.* **26**, 455.
Hugrass, W. N., Jones, I. R., and Phillips, M. G. R. (1981). *J. Plasma Phys.* **26**, 465.
Jones, I. R., and Hugrass, W. N. (1981). *J. Plasma Phys.* **26**, 441.
Kaw, P. K., and Sen, A. (1986). *Nucl. Fusion* (to be published).
Klima, R. (1973). *Plasma Phys.* **15**, 1031.
Klima, R. (1974). *Czech. J. Phys.* B **24**, 846.

Manuscript received 6 November 1985, accepted 13 March 1986